GEOPHYSICAL RESEARCH LETTERS, VOL. 24, NO.13, PAGES 1591-1594, JULY 1, 1997

Two-dimensional seismic image of the San Andreas Fault in the Northern Gabilan Range, central California: Evidence for fluids in the fault zone

C. Thurber[1], S. Roecker[2], W. Ellsworth[3], Y. Chen[2], W. Lutter[1], and R. Sessions[1]

Abstract. A joint inversion for two-dimensional P-wave velocity (Vp), P-to-S velocity ratio (Vp/Vs), and earthquake locations along the San Andreas fault (SAF) in central California reveals a complex relationship among seismicity, fault zone structure, and the surface fault trace. A zone of low Vp and high Vp/Vs lies beneath the SAF surface trace (SAFST), extending to a depth of about 6 km. Most of the seismic activity along the SAF occurs at depths of 3 to 7 km in a southwest-dipping zone that roughly intersects the SAFST, and lies near the southwest edge of the low Vp and high Vp/Vs zones. Tests indicate that models in which this seismic zone is significantly closer to vertical can be confidently rejected. A second high Vp/Vs zone extends to the northeast, apparently dipping beneath the Diablo Range. Another zone of seismicity underlies the northeast portion of this Vp/Vs high. The high Vp/Vs zones cut across areas of very different Vp values, indicating that the high Vp/Vs values are due to the presence of fluids, not just lithology. The close association between the zones of high Vp/Vs and seismicity suggests a direct involvement of fluids in the faulting process.

Introduction

Progress in understanding earthquakes is limited by the lack of in-situ information on physical and chemical properties and processes in active fault zones. One of the ongoing debates is whether the San Andreas fault (SAF) is weak due to high pore-fluid pressures or low fault friction [Lachenbruch and Sass, 1992]. This fundamental uncertainty has led to the proposal to drill into the SAF at seismogenic depths [Hickman et al., 1994]. Geophysical methods are also being used to probe fault zone structure. Fault-zone guided wave (FZGW) studies provide the highest-resolution seismic information about fault zone structure, but at present the models are mostly limited to ones with velocity varying perpendicular to the fault only. Modeling of FZGW's generated by earthquakes and explosions on the SAF [Li et al., 1990; Li et al., 1997] suggests that the fault zone is about 500 m wide, with a 100 to 160 m inner "core layer" and 350 to 400 m "transition layer." Magneto-telluric imaging of the SAF at Parkfield, CA, yields a similar model, with a zone ~500 m wide of very low resistivity extending to a depth of at least 3 km [Unsworth et al., 1997]; the low-resistivity zone is interpreted to be fluid-rich.

The relationship between the SAF surface trace (SAFST) and the seismicity at depth is also uncertain. It has been recognized for over 25 years that the epicenters of most routinely-located earthquakes along the SAF in the Bear Valley to Northern Gabilan Range (NGR) section of the central California tend to lie 2 to 3 km SW of the mapped surface trace of the fault [Brown and Lee, 1971]. Most workers have interpreted this offset as a bias due to the neglect of heterogeneous velocity structure [Boore and Hill, 1973; Ellsworth, 1975; Healy and Peake, 1975; Bakun et al., 1980]. From refraction studies, it is known that the rocks of the NGR (mainly Salinian granites) SW of the SAF have significantly higher velocities than those of the Diablo Range (mainly metamorphosed sedimentary and volcanic rocks) northeast of the SAF [Stewart, 1968; Walter and Mooney, 1982]. In addition, the rocks within the fault zone are slow relative to the surrounding basement rocks [Healy and Peake, 1975; Feng and McEvilly, 1983; Thurber, 1983]. Several studies in the Bear Valley area have shown that the use of station corrections or relatively simple laterally-heterogeneous velocity models can yield relocated epicenters quite close to the SAFST [Boore and Hill, 1973; Ellsworth, 1975; Healy and Peake, 1975; Bakun et al., 1980].

In contrast, Aki and Lee [1976] concluded that the SW offset of epicenters is real, based on a one-step inversion for hypocenters and velocity structure in Bear Valley. The gravity model of Pavoni [1973] in the NGR supports this result, with a SW-dipping boundary between the lower-density rocks of the fault zone and the higher-density Gabilan granites to the SW. One could argue that the one-step nature of the Aki and Lee [1976] inversion and the nonuniqueness of the gravity model of Pavoni [1973] lessen the robustness of these results. However, recent tomography studies in central California also find that the seismicity along the SAF defines a SW-dipping fault [Dorbath et al., 1996; Lin and Roecker, 1997].

We have examined these questions regarding the structure of the SAF and the location of seismic activity with respect to the SAFST using data from a combined passive and active seismic array experiment carried out in the NGR area. An additional motivation for this study is in relation to the proposed program for deep scientific drilling into the SAF [Hickman et al., 1994]. Although this section of the SAF is not the primary candidate for drilling, our study may be useful for designing seismic imaging studies of locked portions of the SAF. The NGR area has the advantage of abundant seismicity that improves our imaging capability, especially with regard to the S-wave velocity structure.

We deployed an array of 48 IRIS-PASSCAL seismic instruments in the NGR area from mid-November 1994 to late May 1995 (Figure 1) for recording of local earthquakes. In addition, we carried out an active seismic experiment in May 1995, consisting of 13 shots and about 200 stations distributed along 3 profiles, plus the passive array sites. This suite of local earthquake and explosion seismograms is used for high-resolution, two-dimensional (2D) imaging of Vp and Vp/Vs structure along the SAF zone.

[1]Dept. of Geology and Geophysics, Univ. of Wisconsin-Madison
[2]Dept. of Earth and Environmental Studies, RPI, Troy, NY
[3]U.S. Geological Survey, Menlo Park, California

Paper number 97GL01435.
0094-8534/97/97GL-01435$05.00

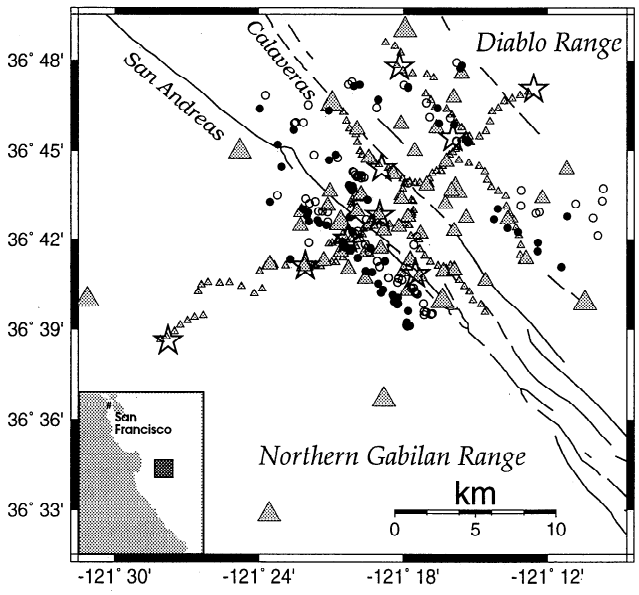

Figure 1. Map of USGS network stations (large triangles), passive array stations (medium triangles), refraction profile sites (small triangles), and shot locations (stars) for the active-source experiment, mapped (solid lines) and inferred (dashed lines) faults, and USGS (open circles) and our final locations (filled circles) for the earthquakes used in the inversion. The index map indicates the study area location.

Inversion Method, Results, and Tests

The modeling approach used is based on the iterative damped-least-squares method of Thurber [1983, 1993] and Evans et al. [1994]. P arrival times and S-minus-P times are inverted for earthquake locations and Vp and Vp/Vs perturbations. We elected to invert for a 2D velocity model oriented normal to the local trend of the SAF for several reasons. The array coverage is elongated in the fault-normal direction (Figure 1) and the local geologic structure varies predominantly in the same direction. Also, our goal was to achieve the highest possible spatial resolution of the structure across the fault zone, at the expense of modeling along-strike variability. Future work will extend the modeling to 3D.

The 2D velocity model had a grid spacing of 1 km near the SAFST and 2 to 3 km elsewhere (Figure 2). A finer grid (0.5 km spacing near the fault) failed to improve the data fit significantly. The 2D Vp model of Thurber et al. [1996], derived from the inversion of explosion P-wave data, was used as a starting model for the joint inversion for Vp, Vp/Vs, and hypocenters, assuming an initial Vp/Vs value of 1.90 (inferred from Wadati diagrams). Data used for the inversion included 4373 P arrival times and 2363 S-minus-P times from 77 earthquakes and 13 explosions (Figure 1). Damping values were selected using a trade-off analysis [Eberhart-Phillips, 1986]. Alternate starting models were also tested; velocity model results differed only in details in low resolution areas, and hypocenter differences were small (~ 100 to 300 m).

The variance reduction achieved by the inversion after 4 iterations was 56%, with a final root-mean-square (RMS) misfit of 0.11 s. The P-wave data were fit better than the S-P data (RMS of 0.07 s versus 0.19 s). Contours of the resolution matrix diagonal elements for Vp and Vp/Vs are shown in Figure 2. Velocity model standard errors were about 1 to 3% , and hypocenter uncertainties ranged from about 20 to 50 m.

The shallow low Vp zone northeast of the SAF reported previously by Thurber et al. [1996] is clearly evident (Figure 2a), extending to a depth of about 3 km. It is interpreted to represent the Hollister trough [Dibblee, 1980]. In addition, a low Vp zone lies beneath the SAFST, extending to about 6 km depth. Most of the seismicity near the SAF lies 1 to 3 km on either side of the SAFST, along the edges of two high Vp bodies. Very little seismic activity is found directly beneath the SAFST. Another cluster of seismicity lies near the Calaveras fault (CF) (6 km NE of the SAFST; Figures 1 and 2a).

Strong variations in Vp/Vs are also evident (Figure 2b). The SAF appears as a zone of high Vp/Vs, dipping steeply to the SW. Most of the seismicity along the SAF lies along the SW edge of this zone. The central part of the model is dominated by a zone of high Vp/Vs (>1.9) that appears to dip NE beneath the Diablo Range. Another zone of seismicity underlies the northeast portion of this Vp/Vs high. Normal Vp/Vs values appear in the NGR to the SW, consistent with its granitic lithology, and in the Diablo Range to the NE, in agreement with Boore and Hill [1973]. The Vp/Vs model correlates well with the geologic interpretation of the area by Dibblee [1980].

A varicty of tests were conducted to assess the robustness of the model. In particular, we were concerned that the sparser array coverage SW of the SAF might be leading to a southwestward bias of the hypocenters near the SAF. The tests included: (a) synthesizing and then inverting arrival-time data sets for hypothetical earthquakes located directly beneath the SAFST as well as at a range of SW offsets (1 to 3 km), (b) inverting the actual data treating the explosions as if they were earthquakes (that is, inverting for their locations rather than holding them fixed), (c) inverting the actual data for the explosions plus just the southwestern group of earthquakes (that is, those lying SW of the SAFST) but applying a constraint to fix the epicenters of these earthquakes to lie at a particular distance from the SAFST (from 0 to 4 km SW). The inversions in test (a) recovered the velocity models and hypocenters quite accurately (velocity values within about 5%, epicenters generally within 100 to 300 m). Thus, if the actual hypocenters had occurred directly beneath the SAFST, our inversion procedure would most likely have located them within a few hundred meters of the fault trace. In test (b), the true explosion epicenters were recovered with an average error of about 200 m; depths errors averaged about 500 m. For test (c), we found that the data were fit best when the epicenters were constrained to lie about 1.8 km SW of the SAFST, with a 95% confidence region extending from 1.5 to 2.1 km SW of the SAFST (determined by an F-test). Taken together, these test results give us confidence that our results are robust.

Discussion and Conclusions

We conclude that most of the seismic activity near the SAF in the Northern Gabilan Range occurs in the depth range of 3 to 7 km in a steeply-dipping zone (~ 70° SW). Projected to the surface, the plane of activity lies within about 400 m of the SAFST. Given the 1-km grid spacing and other uncertainties, the surface projection could certainly intersect the SAFST. This result provides support for the gravity model of Pavoni [1973] that has a low-density zone extending SW of the SAFST, and supports the findings of Dorbath et al. [1996] and Lin and Roecker [1997] that the seismically-defined SAF is SW-dipping in this region. It is also consistent with the suggestion of Unsworth et al. [1997] that the zone of current

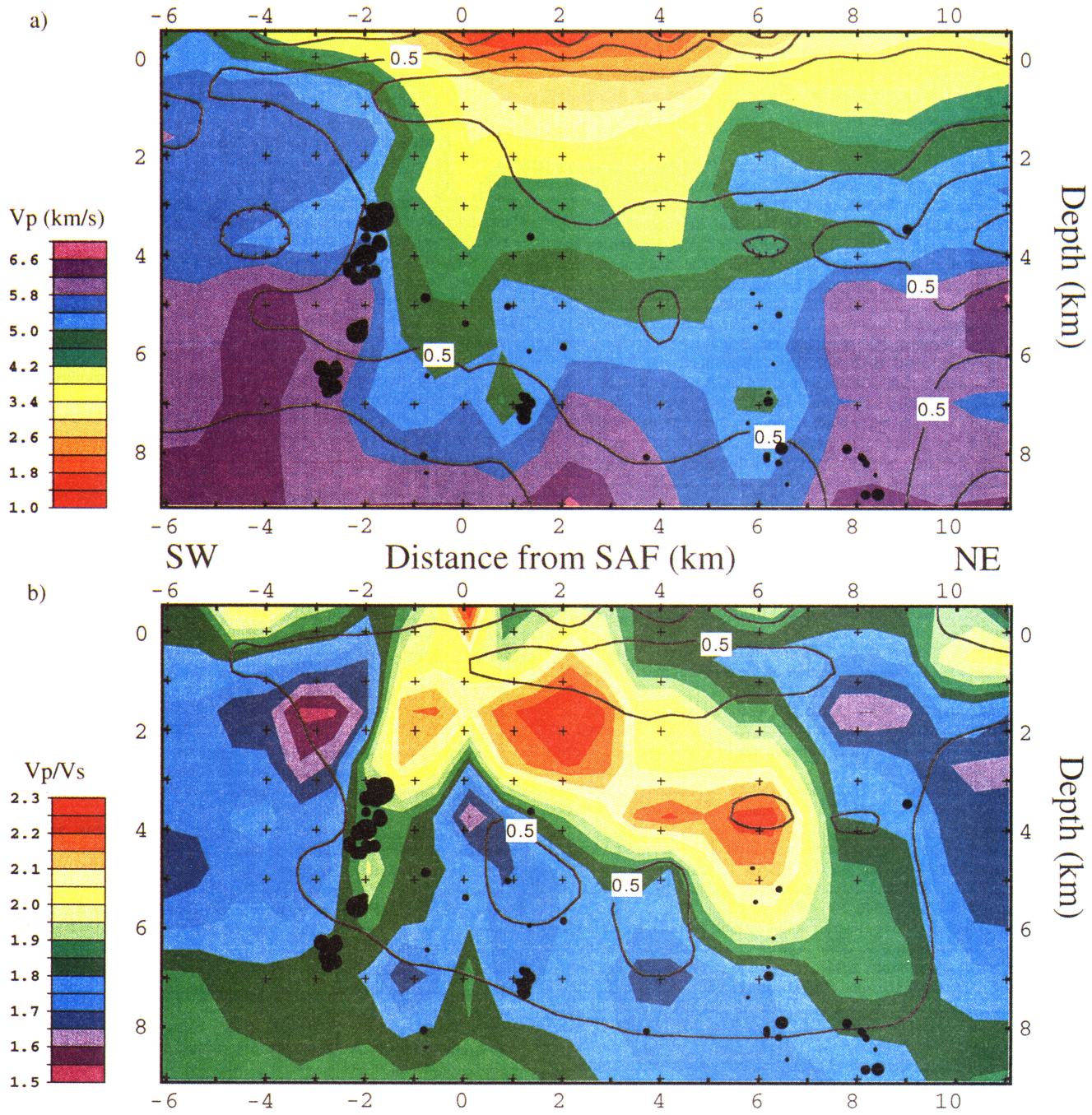

Figure 2. 2D models of (a) Vp and (b) Vp/Vs in a plane normal to the San Andreas fault, with earthquakes included in the inversion indicated by the circles (magnitudes 0.5 to 3.0). Note that the earthquakes are concentrated in areas adjacent to or beneath high Vp/Vs zones. Grid nodes are indicated by '+' and resolution contours are shown (0.25 contour interval).

seismicity and the active surface trace of the SAF at Parkfield, CA, are separated by about 1 km, on opposite sides of a zone of low resistivity.

Unsworth et al. [1997] attribute the low resistivity zone along the SAF at Parkfield to the presence of fluids. Vp/Vs structure can also indicate fluid content [O'Connell and Budiansky, 1974; Eberhart-Phillips et al., 1995; Julian et al., 1996]. One might expect to find earthquake activity within high Vp/Vs zones if high fluid pressures are responsible for the "weakness" of the SAF [Byerlee, 1990; Rice, 1992]. Michelini and McEvilly [1991] found a high Vp/Vs zone (about 2.0) in the vicinity of the hypocenter of the 1966 Parkfield earthquake. We find that the main zone of seismicity lies on the SW edge of a zone of very high Vp/Vs and low Vp (Figure 2). High Vp/Vs values can be due to lithology (e.g., serpentinite [Christensen, 1996]). However, the high Vp/Vs regions in our model cut across substantial Vp variations, making it unlikely that a single lithology is responsible. Our preferred interpretation is that the high Vp/Vs zones represent fluid-rich regions, where the possible sources include

metamorphic fluids [Irwin and Barnes, 1975], sediment dewatering, meteoric water, or fluids rising from the mantle [Rice, 1992]. The juxtaposition of the high-Vp/Vs zones and the zones of seismicity suggests a direct involvement of fluids in the faulting process.

Acknowledgments. We thank M. Unsworth, P. Malin, G. Fuis, and P. Reasenberg for helpful reviews. Discussions with Donna Eberhart-Phillips are gratefully acknowledged. This project was funded by the Continental Dynamics program of the National Science Foundation under grants EAR-9317030 (UW) and EAR-9316733 (RPI), and by the Deep Continental Studies program of the USGS. The instruments used in the field program were provided by the PASSCAL facility of the Incorporated Research Institutions for Seismology (IRIS) through the Lamont and Stanford Instrument Centers. The facilities of the IRIS Consortium are supported by the National Science Foundation under Cooperative Agreement EAR-9023505. We thank the PASSCAL personnel for many hours of assistance. USGS network data were obtained from the Northern California Data Center. We are grateful to the area landowners for permission to deploy the array and carry out the active experiment, and to T. Burdette for assistance with permitting. We also thank the many people from UW-Madison, RPI, the USGS, and ETH-Zurich who helped in the field. GPRC contribution No. 575.

References

Aki, K. and W. H. K. Lee, Determination of three-dimensional velocity anomalies under a seismic array using first P arrival times from local earthquakes, I, A homogeneous initial model, *J. Geophys. Res., 81*, 4381-99, 1976.

Bakun, W. H., R. M. Stewart, C. G. Bufe, and S. M. Marks, Implications of seismicity for failure of a section of the San Andreas fault, *Bull. Seism. Soc. Am., 70*, 185-201, 1980.

Boore, D. M., and D. P. Hill, Wave propagation characteristics in the vicinity of the San Andreas fault, in *Proc. Conf. Tectonic Problems of the San Andreas Fault System, Stanford Univ. Pub. Univ. Ser., Geol. Sci., 13*, 215-224, 1973.

Brown, R. D., Jr., and W. H. K. Lee, Active faults and preliminary earthquake epicenters (1969-1970) in the southern part of the San Francisco Bay region, *U. S. Geol. Surv. Map MF-307*, 1971.

Byerlee, J, Friction, overpressure, and fault normal compression, *Geophys. Res. Lett., 17*, 2109-2112, 1990.

Christensen, N. I., Poisson's ratio and crustal seismology, *J. Geophys. Res., 101*, 3139-3156, 1996.

Dibblee, T., Geology along the San Andreas fault from Gilroy to Parkfield, in *San Andreas Fault Zone in Northern California*, edited by R. Streitz and R. Scherburne, *CDMG Special Rep. 140*, pp. 3-18, 1980.

Dorbath, C., D. Oppenheimer, F. Amelung, and G. King, Seismic tomography and deformation modeling of the junction of the San Andreas and Calaveras faults, *J. Geophys. Res., 101*, 27,917-27,941, 1996.

Eberhart-Phillips, D., Three-dimensional velocity structure in northern California Coast Ranges from inversion of local earthquakes arrival times, *Bull. Seismol. Soc. Am., 76*, 1025-1052, 1986.

Eberhart-Phillips, D., W. D. Stanley, B. D. Rodriguez, and W. J. Lutter, Surface seismic and electrical methods to detect fluids related to faulting, *J. Geophys. Res., 100*, 12,919-12,936, 1995.

Ellsworth, W. L., Bear Valley, California, earthquake sequence of February-March 1972, *Bull. Seism. Soc. Am., 65*, 483-506, 1975.

Ellsworth, W. L., Characteristic earthquakes and long-term earthquake forecasts: Implications of central California seismicity, in F. Y. Cheng and M. S. Sheu, *Urban Disaster Mitigation: the Role of Science and Technology*, Elsevier, pp. 1-14, 1995.

Evans, J. R., D. Eberhart-Phillips, and C. H. Thurber, User's manual for SIMULPS12 for imaging Vp and Vp/Vs: a derivative of the Thurber tomographic inversion SIMUL3 for local earthquakes and explosions, *U.S. Geol. Surv. Open File Rep. OFR 94-431*, 101 pp., 1994.

Feng, R., and T. V. McEvilly, Interpretation of seismic reflection profiling data for the structure of the San Andreas fault zone, *Bull. Seismol. Soc. Am., 73*, 1701-1720, 1983.

Healy, J. H., and L. G. Peake, Seismic velocity structure along a section of the San Andreas fault near Bear Valley, California, *Bull. Seismol. Soc. Am., 65*, 1177-1197, 1975.

Hickman, S., M. Zoback, L. Younker, and W. Ellsworth, Deep scientific drilling in the San Andreas fault zone, *EOS Trans. AGU, 75*, 137, 1994.

Irwin, W. P., and I. Barnes, Effect of geologic structure and metamorphic fluids on the seismic behavior of the San Andreas fault system in central and northern California, *Geology, 3*, 713-716, 1975.

Julian, B.R., A. Ross, G.R. Foulger, and J.R. Evans, Three-dimensional seismic image of a geothermal reservoir: The Geysers, CA, *Geophys. Res. Lett., 23*, 685-688, 1996.

Lachenbruch, A. H., and J. H. Sass, Heat flow from Cajon Pass, fault strength and tectonic implications, *J. Geophys. Res., 97*, 2005-2012, 1992.

Li, Y., P. Leary, K. Aki, and P. E. Malin, Seismic trapped modes in the Oroville and San Andreas fault zones, *Science, 249*, 763-766, 1990.

Li, Y.-G., W. L. Ellsworth, C. H. Thurber, P. Malin, and K. Aki, Fault-zone guided waves from explosions in the San Andreas fault at Parkfield and Cienega Valley, California, *Bull. Seismol. Soc. Am., 87*, 210-221, 1997.

Lin, C. H., and S. W. Roecker, Three-dimensional P-wave velocity structure of the Bear Valley region of central California, *Pageoph*, in press, 1997.

Michael, A. J., and D. Eberhart-Phillips, Relations among fault behavior, subsurface geology, and three-dimensional velocity models, *Science, 253*, 651-654, 1991.

O'Connell, R. J., and Budiansky, B., Seismic velocities in dry and saturated cracked solids, *J. Geophys. Res., 79*, 5412-5426, 1974.

Pavoni, N., A structural model for the San Andreas fault zone along the northeast side of the Gabilan Range, in Proc. Conf. Tectonic Problems of the San Andreas Fault System, *Stanford Univ. Pub. Univ. Ser., Geol. Sci., 13*, 259-267, 1973.

Stewart, S. W., Preliminary comparison of seismic traveltimes and inferred crustal structure adjacent to the San Andreas fault in the Diablo and Gabilan ranges of central California, in Proc. Conf. Geologic Problems of the San Andreas Fault System, *Stanford Univ. Pub. Univ. Ser., Geol. Sci., 11*, 218-230, 1968.

Rice, J. R., Fault stress states, pore pressure distributions, and the weakness of the San Andreas fault, in *Fault Mechanics and Transport Properties of Rocks*, B. Evans and T.-F. Wong (eds.), Academic Press, New York, pp. 475-503, 1992.

Thurber, C. H., Earthquake locations and three-dimensional crustal structure in the Coyote Lake area, central California, *J. Geophys. Res., 88*, 8226-8236, 1983.

Thurber, C. H., Local earthquake tomography: Velocities and Vp/Vs - theory (invited chapter), in *Seismic Tomography*, H. M. Iyer and K. Hirahara (eds.), Chapman and Hall, pp. 563-583, 1993.

Thurber, C., S. Roecker, W. Lutter, and W. Ellsworth, Imaging the San Andreas fault with explosion and earthquake sources, *Eos Trans. AGU, 77*, 45-58, 1996.

Unsworth, M., P. Malin, G. Egbert, and J. Booker, Internal structure of the San Andreas fault at Parkfield, CA, *Geology*, 359-362, 1997.

Walter, A. W., and W. D. Mooney, Crustal structure of the Diablo and Gabilan ranges, central California: a reinterpretation of existing data, *Bull. Seismol. Soc. Am., 72*, 1567-1590, 1982.

C. Thurber, W. Lutter, and R. Sessions, Dept. of Geology and Geophysics, UW-Madison, 1215 W. Dayton St., Madison, WI 53706

S. Roecker and Y. Chen, Dept. of Earth and Environmental Studies, Rensselaer Polytechnic Institute, Troy, NY 12180

W. Ellsworth, U.S. Geological Survey, Menlo Park, CA 94025

(Received February 24, 1997; accepted April 17, 1997)